Crystallization and Electrical Properties of SBN60 Thin Films Prepared by Ion Beam Sputter Deposition

Jae-Hoon Jang, Seong-Won Jeong, and Hee Young Lee[a]
Department of Materials Science and Engineering, Yeungnam University, Dae-dong, Gyeongsan-si, Gyeongsangbuk-do 712-749, Korea

[a] E-mail : hyulee@yu.ac.kr

(Received July 28 2004, Accepted December 28 2004)

$Sr_{0.6}Ba_{0.4}Nb_2O_6$, hereafter SBN60, thin films of 300 nm thickness were deposited using ion beam sputtering technique, in which sintered ceramic target of the same composition was utilized and the $Ar:O_2$ gas ratio was controlled during deposition onto $Pt(100)/TiO_2/SiO_2/Si$ substrate. Crystallization and orientation behavior as well as electrical properties of the films were examined after annealing treatment at 650~800 °C. It was found that the film orientation was dependent upon $Ar:O_2$ ratio, in which strong (001) orientation was developed when the gas ratio was about 1:4 at 4.3×10^{-4} torr. Typical remanent polarization (2Pr), the coercive field (Ec) and the dielectric constant of Pt/SBN60/Pt thin film capacitor were approximately 10 $\mu C/cm^2$, 60 kV/cm, and 615, respectively.

Keywords : SBN, Ion beam sputtering, Ferroelectric thin film, Tungsten bronze structure

1. INTRODUCTION

$Sr_xBa_{1-x}Nb_2O_6$, hereafter SBN, is a solid solution between $BaNb_2O_6$ and $SrNb_2O_6$, which crystallizes in the tetragonal tungsten bronze-type structure[1] in the composition $0.25 \leq x \leq 0.75$. The SBN ceramics have been extensively studied for possible technological applications in electro-optic, pyroelectric, piezoelectric and photorefractive devices due to its excellent pyroelectric and linear electro-optic effects with low half-wave voltage and photorefractive sensitivity[2-4]. In addition, it has the advantage of lead-free composition that concerned with environment, safety and health.

The SBN crystallizes in a tetragonal tungsten bronze structure with the space group P4bm[5] containing five formula units per unit cell. Figure 1 shows a schematic of the tungsten bronze structure along the *c*-axis, *i.e.* the direction of spontaneous polarization[6]. The common formula of the tungsten bronze structure can be described as $(A1)_2(A2)_4(C)_4(B1)_2(B2)_8O_{30}$. The skeletal framework of this structure is formed by BO_6 octahedra. These octahedra share corners to form cavities around the A1, A2, and C sites. The axes of these octahedra are slightly tilted to the *c*-axis, depending on the chemical composition of the solid solution. In SBN, Sr ions are located on the A1 and A2 sites whereas Ba ions are located only on the A2 site because of the relatively larger ionic radius. Since there are only five Sr and Ba ions in a unit cell, one of the six A1 and A2 sites is vacant, while the B1 and B2 sites are fully occupied by Nb ions, the C sites may contain only ions with smaller ionic radius and are therefore not occupied in SBN[7].

Various processes have been attempted in order to prepare SBN thin films, including sol-gel, metalorganic decomposition (MOD), pulsed laser deposition and rf magnetron sputtering[8-15].

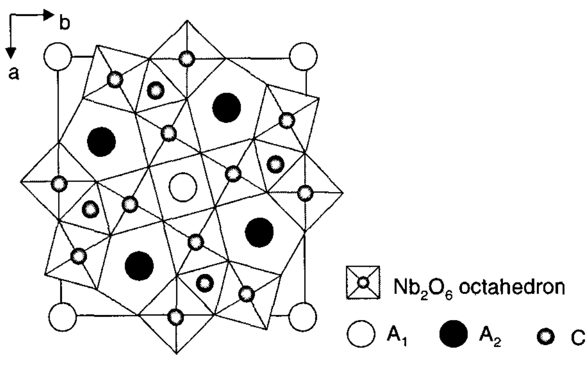

Fig. 1. Atomic arrangement in a unit cell of a tungsten-bronze type structure projected along the *c*-axis(after P. B. Jamieson et al.).

Since 1979, ion beam sputter deposition (IBSD) has been used to deposit various multi-component oxide thin films, such as PZT and $YBa_2Cu_3O_{7-x}$[16]. The advantage of IBSD over conventional sputtering techniques includes low deposition pressure, excellent adhesion to the substrate due to high kinetic energy ion beams, and the easier control of stoichiometry if multiple sources are adopted.

In this paper, the SBN thin films are prepared by IBSD on Pt coated silicon wafers. The effects of preparation parameters such as $Ar:O_2$ ratio, working pressure, annealing temperature on crystallization behavior and electronic properties of $Sr_{0.60}Ba_{0.40}Nb_2O_6$ (SBN60) thin films are discussed.

2. EXPERIMENTAL PROCEDURE

SBN60 thin films were deposited using IBSD technique utilizing the ceramic target of the same composition that was prepared by the conventional solid-state sintering of uniaxially pressed mixed-oxide disk. $Pt(100)/TiO_2/SiO_2/Si(100)$ wafer with 200 nm thick platinum layer was used as a substrate, which was heated to 400 °C, and the mixture of argon and oxygen gas was introduced to the chamber during deposition. After the deposition, samples were given annealing treatment at 650~800 °C in air. The details of thin film preparation conditions are summarized in Table 1.

Surface morphology and crystallization behavior were examined using FE-SEM (S-4200, Hitachi, Japan), and XRD (D/MAX-2500, Rigaku, Japan) with thin film sample attachment.

Leakage current, ferroelectric hysteresis, and C-V curve characteristics were measured utilizing Keithley 617 electrometer, RT66A ferroelectric tester with Sawyer-Tower circuit operated at 1 kHz, and HP4192A impedance analyzer for the samples with platinum top electrode deposited through shadow mask by ion beam sputtering.

Table 1. Summary of deposition parameters.

Target	$Sr_{0.6}Ba_{0.4}Nb_2O_6$ (SBN60)
Substrate	$Pt(100)/TiO_2/SiO_2/Si(001)$
Base Pressure	1.0×10^{-6} Torr
Working Pressure	$1.0 \sim 8.9 \times 10^{-4}$ Torr
Discharge Power	400 V, 0.4 A
Beam Power	1 kV, 40 mA
Accelerator Power	0.1 kV, 2 A
Deposition Temperature	400 °C
P_{O2} / P_{Ar}	0 ~ 7.9

3. RESULTS AND DISCUSSION

3.1 Crystallization and film orientation

Figure 2 shows the XRD patterns of SBN60 thin films deposited on $Pt(100)/TiO_2/SiO_2/Si(100)$ substrate. The films shown in Fig. 2(a) were grown under different working pressure and $Ar:O_2$ ratio followed by annealing treatment at 750 °C for 30 minutes, while the films in Fig. 2(b) were grown at the fixed working pressure of 4.3×10^{-4} torr which corresponded to $Ar:O_2$ ratio of 1:4 and annealed at different temperatures in the range 650 ~ 800 °C. From the XRD patterns, it is clear that the films were composed of tetragonal tungsten bronze phase with no secondary phases. It is also evident that the films were textured along (001) planes, in which the degree of orientation varied with working pressure and $Ar:O_2$ ratio as well as the annealing temperature. It is noted that the strongest reflection peak in case of SBN ceramic, i.e. (311) peak, is well suppressed. Similar finding was reported for SBN25 thin films prepared by rf magnetron sputtering[14]. However, (001) texturing for SBN films with higher Sr content has not reported yet. The best results were obtained when the film was deposited under the working pressure of 4.3×10^{-4} torr and annealed at 750 °C for 30 minutes in air.

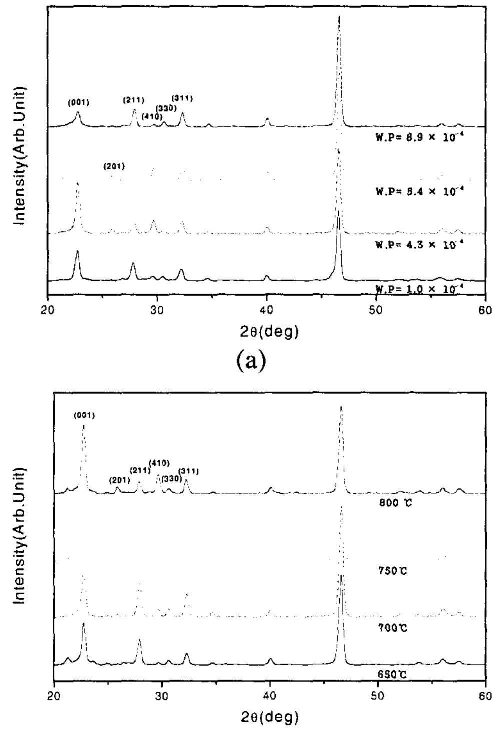

Fig. 2. X-ray diffraction patterns of SBN60 thin films on $Pt(100)/TiO_2/SiO_2/Si(100)$ substrate: (a) deposited at varying working pressure with annealing at 750 °C and (b) deposited at constant working pressure of 4.3×10^{-4} torr with annealing at different temperatures.

3.2 Microstructure analysis

Figure 3 shows FE-SEM micrographs of SBN60 films. The film thickness as determined from the cross-sectional photograph was about 300 nm. It is seen that grain growth occurred, as expected, with the increase of annealing temperature. The analysis of chemical composition of the film was attempted by energy-dispersive X-ray analyzer (Horiba, EX-300) by comparing EDS spectra of target and films, and the film composition was regarded about the same as the composition of the target within the error limit of the analysis.

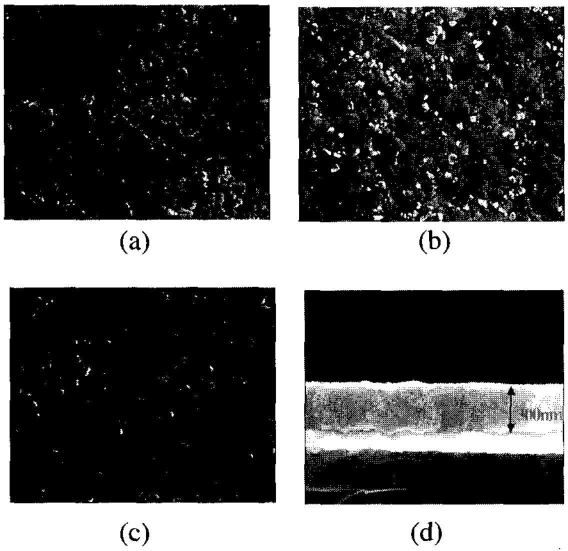

Fig. 3. Scanning electron micrographs of SBN60 thin films deposited at the constant working pressure of 4.3 x 10^{-4}: (a) 700 °C, (b) 750 °C, (c) 800 °C, and (d) cross-section of (b).

3.3 Electrical properties

I-V curves of the Pt/SBN60/Pt thin film capacitor samples annealed at 750 °C are depicted in Fig. 4. The leakage current density level below the electric field of 50 kV/cm is on the order of 10^{-7} A/cm^2 when the top Pt electrodes were biased to positive voltage.

Ferroelectric hysteresis behavior was also measured as illustrated in Fig. 5 for thin film capacitor sample deposited at the total working pressures of 4.3 x 10^{-4} torr and 5.4 x 10^{-4} torr followed by annealing at 750 °C in air, respectively. It is seen that well-saturated loops were observed with remanent polarization (2Pr) value of about 11 μC/cm^2 and 10 μC/cm^2, coercive field (Ec) of 65 kV/cm and 60 kV/cm, respectively. These values compare favorably with the reported data for the SBN films prepared by other processes where 2Pr value ranges from 2 to 50 μC/cm^2 and Ec value from 5 to 200 kV/cm[7,8,16]. The rather smaller 2Pr and Ec values might indicate the films were not fully textured along *c*-axis. It is worth mentioning, however, that these values are better than the ones obtained for *c*-axis oriented SBN25 films deposited by rf magnetron sputtering[14].

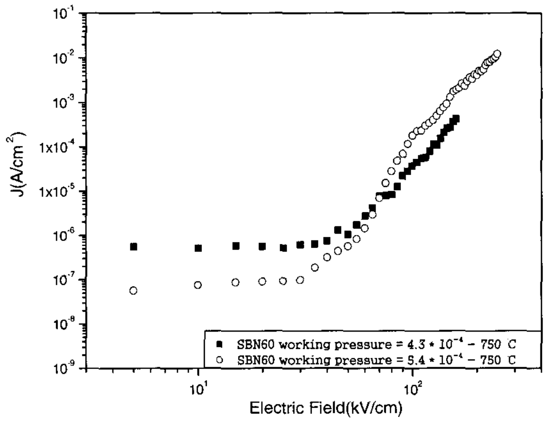

Fig. 4. Leakage current versus applied electric field for Pt/SBN60/Pt thin film capacitor.

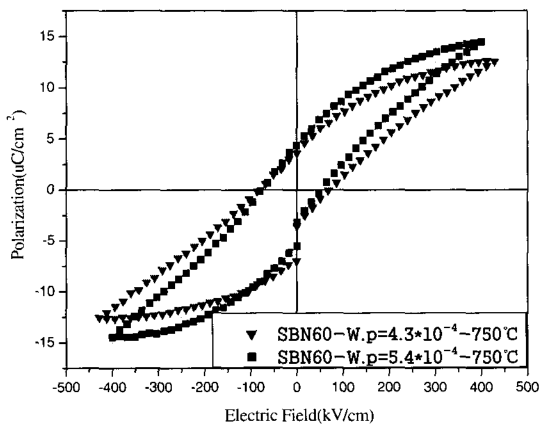

Fig. 5. P-E hysteresis behavior for Pt/SBN/Pt capacitor.

4. CONCLUSION

Highly *c*-axis oriented SBN60 thin films with 300 nm thickness were obtained using ion beam sputtering onto Pt(100)/TiO_2/SiO_2/Si(100) wafers followed by annealing treatment at 650~800 °C in air. The orientation behavior showed dependence on working pressure and Ar:O_2 ratio as well as annealing temperature with the best result obtained at 4.3 x 10^{-4} torr, 1:4 gas ratio, and 750 °C. The films were composed of tetragonal tungsten bronze phase as analyzed from the XRD patterns. Measured electrical properties of Pt/SBN60/Pt thin film capacitor were as follows: remnant polarization (2Pr) value was approximately 10 μC/cm^2, the coercive field (Ec) 60 kV/cm, and the dielectric constant 615, respectively.

ACKNOWLEDGMENT

This work was supported by the Basic Research Program of the Ministry of Information and Communication(Project No. 2003-1-00964).

REFERENCES

[1] Y. Xu, "Ferroelectric materials and their application", North Holland, Amsterdam, p. 254, 1991.

[2] M. D. Ewbank, R. R. Neurgaonkar, W. k. Cory, and J. Feinberg, "Photorefractive properties of strontium-barium niobate", J. Appl. Phys., Vol. 62(2), p. 374, 1987.

[3] R. B. Maciolek and S. T. Liu, "Preparations and properties of low loss $Sr_{1-x}Ba_xNb_2O_6$ ferroelectric single crystals", J. Electron. Mater., Vol. 2, No. 2, p. 191, 1973.

[4] R. R. Neurgaonkar, M. H. Kalisher, T. C. Lim, E. J. Staples, and K. I. Keester, "Czochralski single crystal growth of $Sr_{0.61}Ba_{0.39}Nb_2O_6$ for surface acoustic wave applications", Mater. Res. Bull., Vol. 15, No. 9, p. 1235, 1980.

[5] P. B. Jamieson, S. C. Abrahams, and J. L. Bernstein, "Ferroelectric tungsten bronze-type crystal structures. I. Barium strontium niobate $Ba_{0.27}Sr_{0.75}Nb_2O_{5.78}$", J. Chem. Phys., Vol. 48, No. 11, p. 5048, 1968.

[6] K. H. Hellwege and A. M. Hellwege(eds.), "Landolt-bornstein new series", Group lll, Vol. 28a, p. 148, 1988.

[7] M. P. Trubelja, E. Ryba, and D. K. Smith, "A study of positional disorder in strontium barium nibate", J. Mater. Sci., Vol. 31, No. 6, p. 1435, 1996.

[8] Y. Xu, C. J. Chen, R. Xu, and J. D. Mackenzie, "Ferroelectric $Sr_{0.6}Ba_{0.3}Nb_2O_6$ thin film by the sol-gel process: Electrical and optical properties", Phys. Rev. B, Vol. 44, No. 1, p. 35, 1991.

[9] S. S. Thöny, K. E. Youden, J. S. Harris, Jr., and L. Hesselink, "Growth of epitaxial strontium barium niobate thin film by pulsed laser deposition", Appl. Phys. Lett., Vol. 65, No. 16, p. 2018, 1994.

[10] K. Tanaka, O. Nakagawara, M. Nakano, T. Shimuta, H. Tabata, and T. Kawai, "Epitaxial growth of (Sr, Ba)Nb_2O_6 thin films by pulsed laser deposition", Jpn. J. Appl. Phys., Vol. 37, No. 11, p. 6142, 1998.

[11] C. H. Luk, M. M. T. Ho, C. L. Mak, K. J. Wong, and G. K. H. Pang, "Fabrication and structural properties of sol–gel derived SBN films", J. Eur. Ceram. Soc., Vol. 19, No. 6-7, p. 1443, 1999.

[12] C.-A. Jong and J.-Y. Gan, "Crystallization of $Sr_{0.5}Ba_{0.5}Nb_2O_6$ thin films on $LaNiO_3$ electrodes by RF magnetron reactive sputtering", Jpn. J. Appl. Phys., Vol. 39, No. 2A, p. 545, 2000.

[13] J. Koo, J. H. Jang, and B.-S. Bae, "Preparation and characteristics of seeded epitaxial (Sr,Ba)Nb_2O_6 optical waveguide thin films using sol-gel method", J. Mat. Res., Vol. 16, No. 2, p. 430, 2001.

[14] M. K. Ryu, S. H. Lee, H. J. Joo, J. P. Kim, M. S. Jang, and Y. S. Yang, "Electronic defect characteristic of ferroelectric $Sr_{0.25}Ba_{0.75}Nb_2O_6$ thin films", Ferroelectrics, Vol. 260, No. 1-4, p. 99, 2001.

[15] D. G. Lee, H. W. Lee, H. Y. Lee, J.-J. Kim, and S.-H. Cho, "The crystallization behavior of (Sr,Ba) Nb_2O_6 thin films prepared by a hybrid metalorganic decomposition", Ferroelectrics, Vol. 270, p. 33, 2002.

[16] C. A. P. de Araujo, J. F. Scott, and G. W. Taylor (eds.), "Ferroelectric Thin Films: Synthesis and Basic Properties", Gordon and Breach, New York, p. 393, 1996.